17th World Conference on Earthquake Engineering, 17WCEE

Sendai, Japan - September 27th to October 2nd, 2021

INFLUENCE OF MAXWELL STIFFNESS IN SEISMIC RESPONSE OF FRAMES EQUIPPED WITH VISCOUS DAMPERS

J. Conde[(1)], A. Bernabeu[(2)]

[(1)] *Universidad Politécnica de Madrid, jorge.conde@upm.es*
[(2)] *Universidad Politécnica de Madrid,alejandro.bernabeu@upm.es*

Abstract

Added viscous damping systems improve the seismic resiliency of structures through a reduction of key variables related to damage. These systems can be mathematically represented by a serial combination of a linear spring and a non-linear dashpot. The spring stiffness, referred to as Maxwell stiffness, is dominated by the most flexible element of the set, including brace extender, auxiliary mounting hardware and the damper itself. Existing experimental data are used hereby to show that the actual stiffness is a reduced fraction (between 0.25 and 0.50) of the value generally adopted in design, based solely on the brace extender properties. A numerical study involving a 3- and a 5- storey frames equipped with different viscous damping systems, indicates that this stiffness reduction results in a very large increase in structural damage (measured by the plastic strain energy dissipated by the main structure), and a large increase in total acceleration. Additionally, in the 5-storey frame, residual drift ratio and drift ratio show a large to moderate sensitivity to the Maxwell stiffness. These results suggest that, on the absence of accurate experimental information, the Maxwell stiffness used for analysis and damage estimation should be conservatively taken as a fraction (between 0.25 and 0.50, approximately) of the stiffness based on brace extender properties and centerline length. Due to the scarcity of experimental data used, these conclusions must be considered as preliminary.

Keywords: viscous dampers; Maxwell stiffness; damper stiffness; damage control.

1. Introduction

Traditional earthquake-resistant design is based on a trade-off between acceptable damage and survivability. In recent years, catastrophic events (Northridge, USA, 1994; Kobe, Japan, 1995; Chile, 2010; Christchurch, New Zealand, 2011; etc.) demonstrated that design prescriptions, although effective for life-safety purposes, must be improved to reduce post-event trauma and economical losses. Thus, the current research effort is largely shifted towards resiliency and enhanced seismic performance [1]. In this context, inclusion of supplemental viscous damping systems in buildings is widely recognized as an effective mean to reduce structural damage, mainly by dissipating seismic energy input through viscous mechanisms rather than hysteresis [2][3]. Added viscous damping reduces interstorey drift, thus minimizing or even avoiding plastic excursions, but also reducing damage to non-structural elements, a key aspect in resiliency considerations. Other important benefits are a significant reduction of floor accelerations, crucial for secondary systems, and, under certain circumstances, a reduction of residual drift [4][5].

Damping systems can be effectively represented by a Maxwell model, defined by stiffness and viscous damping [6]. Besides the damper unit, the brace extender is the most conspicuous element in the set, and the only one not dependent on proprietary data. Current engineering procedures estimate the Maxwell stiffness based solely on this element, neglecting the important contribution of other auxiliary mounting elements and the damper unit itself [7][8]. Moreover, simplified procedures in ASCE SEI-7/16 are based on the reduction of the Maxwell model to a pure dashpot, which is equivalent to the assumption of infinite stiffness [9]. Rules of thumb have been proposed to determine reasonable values of stiffness that allegedly allow such simplifications. However, recent experimental [10][11] and analytical [12] studies have shown that the limited stiffness of the damping system exerts a significant influence on the structural performance of structures equipped with these systems.

Data obtained from existing state-of-the-art tests are used to explore the flexibility induced by auxiliary elements in the damping system. It is shown that the reduced stiffness falls approximately between 25% - 50% of the one calculated purely on the basis of the brace extender element. The implications of this increased flexibility are then explored analyzing two different steel frames equipped with a variety of viscous damping systems, with three different levels of reduction of the Maxwell stiffness. The results show that damage-related variables exhibit a considerable sensitivity to this reduction, suggesting that the Maxwell stiffness considered for analysis should be conservatively reduced, unless accurate information is made available. Given the scarcity of experimental data, these results must be considered as preliminary.

2. Reduction of Maxwell stiffness due to component flexibility

Fig. 1(a) shows a typical damping set, formed by several elements: damping unit, brace extender and other auxiliary elements (gusset plates, cleats, frontal plates, bolts, clevises, etc.) connecting the damper to the brace and main structure. The corresponding mathematical model is shown in Fig. 1(b). The damper is characterized by its damping coefficient c_b and damper exponent a, and constitutes the viscous component (subscript 'b' indicates properties referred to brace axis). All other elements in the set contribute to the overall stiffness k_b; for this serial arrangement:

$$k_b^{-1} = k_{bo}^{-1} + k_{bb}^{-1} + k_{bd}^{-1}, \tag{1}$$

where k_{bb} is the stiffness of the brace extender, k_{bd} is the stiffness of the damper unit and k_{bo} the equivalent stiffness of the additional mounting hardware. Although the damper and auxiliary element stiffnesses k_{bd} and k_{bo} are limited, in practical applications they are generally assumed as very large. Then, by Eqn. (1) $k_b \approx k_{bb}$, with k_{bb} often calculated on the basis of the centerline length. It is worth mentioning, however, that the value of k_b in Eqn. (1) will be dominated by the most flexible element in the set. This is illustrated in Fig. 1(c)

where k_b is plotted as a function of k_{bo} and k_{bb} (assuming $k_{bd} = \infty$). Thus, selection of a very stiff brace element does not ensure high values of k_b, unless k_{bd} and k_{bo} are of a similar order of magnitude.

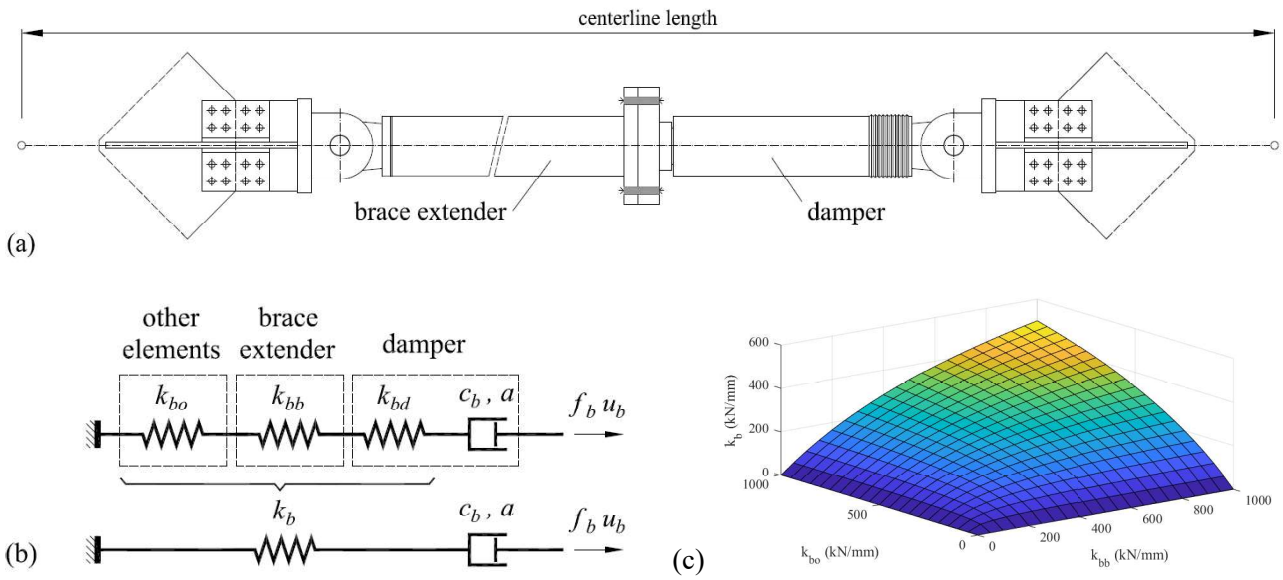

Fig. 1 – Damper set; (a) typical arrangement; (b) analytical model; (c) global stiffness k_b as a function of k_{bb} and k_{bo}, assuming $k_{bd} = \infty$.

Accurate measures of real-scale damping set properties including auxiliary hardware elements (clevises and brackets) were performed in the Tokyo Institute of Technology, Japan [10]; Table 1 lists the corresponding experimental values, reported by Akcelyan *et al* [12]. In the Table, k_{bb} has been calculated as $A_b \cdot E/L_b$, where E is the Young modulus of steel (200 GPa), A_b the brace extender cross-section, and L_b the actual brace extender length; k_{bo} has been found using Eqn. (1); and k_{bb}* has been estimated as $A_b \cdot E/L$, where L is the centerline length of the set as shown in Fig. 1(a), and corresponds with the approximate Maxwell stiffness considered in practical calculations. The table shows also direction of installation (X, Y), fundamental period T of the structure for the corresponding direction, damping coefficient c_b and damper exponent a. The last column shows that the actual stiffness k_b falls between 13% and 28% of the stiffness usually adopted in design k_{bb}*, a very remarkable deviation.

Table 1 – Properties of non-linear viscous damping systems (after Akcelyan *et al* [12]).

Direction	*T*	*Storey*	*L*	L_b	A_b	c_b	*a*	k_{bd}	k_{bb}	k_{bo}	k_b	k_{bb}*	k_b/k_{bb}*
	s		mm	mm	mm2	kN·(s/mm)$^{0.38}$	-	kN/mm	kN/mm	kN/mm	kN/mm	kN/mm	-
		4-3	4,025	2,429	9,121	49	0.38	119	*751*	*144*	60	*453*	*13%*
X	0.536	2	3,947	2,104	8,380	98	0.38	193	*797*	*315*	104	*425*	*24%*
		1	4,706	2,864	8,380	98	0.38	193	*585*	*332*	101	*356*	*28%*
		4-3	3,947	2,104	8,380	98	0.38	193	*797*	*315*	104	*425*	*24%*
Y	0.575	2	3,849	1,542	15,323	196	0.38	438	*1,987*	*357*	179	*796*	*22%*
		1	4,629	2,322	15,323	196	0.38	438	*1,320*	*356*	171	*662*	*26%*

[1]Data in italics (k_{bb}, k_{bo}) has been inferred. For explanation of symbols refer to main text.

If the centerline length of the bracing system L is replaced by a longer length L', but similar damper forces are assumed, the damper unit and the auxiliary elements remain unchanged. Thus, k_{bd} and k_{bo} are unchanged, the brace length is increased to $L_b' = L' - (L-L_b)$ and k_{bb}, k_b, k_{bb}* can be recalculated accordingly; the ratio k_b/k_{bb}* takes values between 23% and 40%. In this calculation, the brace element has been assumed unchanged; however, buckling considerations would probably result in a larger cross-sectional area A_b'. In that case the k_b/k_{bb}* ratios would decrease further; for instance, assuming $A_b' = 2 \cdot A_b$, the corresponding ratios lie between 13% and 24%.

For linear dampers there exists (to these authors' knowledge) no similar data to those in Table 1. This is probably due to their current limited applicability in seismic design. Thus, in order to obtain a range of magnitude for k_b/k_{bb}*, certain assumptions and simplifications are adopted hereby: i) non-linear dampers in Table 1 are replaced by linear dampers with similar damper forces, leading to an identical choice of auxiliary elements and brace extender; ii) damper forces (not listed in the original reference) are derived from peak drift velocity values v_0 obtained from peak drift ratios θ assuming harmonic vibration at natural period T; iii) a conservative value of relaxation time λ (= $c_{b,1}/k_d$) is assumed for linear dampers. v_0 is derived from basic dynamic considerations as $v_0 \approx 2\pi\theta h/T$, where h is the storey height. Recalling that peak damper force in a viscous damper is given by $c_b \cdot v_0^a$:

$$c_{b,1} v_0 = c_{b,a} v_0^a, \tag{2}$$

where $c_{b,1}$ and $c_{b,a}$ are damping coefficients for the linear and non-linear damper, respectively. Thus, using Eqn. (2), the value of $c_{b,1}$ can be established. The damper stiffness k_d can then be found as $c_{b,1}/\lambda$. Values of λ are reported in references [13]-[15], ranging between λ = 0.006s and 0.014s; larger values are observed for larger damping coefficients $c_{b,1}$; the minimum value (0.006) is conservatively adopted. The corresponding results are shown in Table 2, where k_{bb}, k_{bo} and k_{bb}* are taken from Table 1, and k_b is obtained from Eqn. (1). The ratios k_b/k_{bb}* are on the range 19%-42%, slightly larger than those for non-linear dampers. If the relaxation time is taken as 10 times shorter (0.0006s) results in a 26%-57% range, whereas a relaxation time 10 times larger (0.06s) results in 6%-12% range. On the absence of accurate information, the range shown in the table is adopted as a reference for the analysis performed in the next Section.

Table 2 – Properties assumed for linear viscous damping systems.

Dir.	T	*Storey*	θ	h	v_0	f_b	$c_{b,1}$	λ	k_{bd}	k_{bb}	k_{bo}	k_b	k_{bb}*	k_b/k_{bb}*
	s		%	mm	mm/s	kN	kN·(s/mm)	s	kN/mm	kN/mm	kN/mm	kN/mm	kN/mm	-
X	0.536	4	0.54	3000	189	359	1.90	0.006	316	751	144	88	453	19%
		3	0.56	3000	198	365	1.85	0.006	308	751	144	87	453	19%
		2	0.64	3000	225	768	3.41	0.006	568	797	315	161	425	38%
		1	0.62	3485	253	803	3.17	0.006	528	585	332	151	356	42%
Y	0.575	4	0.65	3000	213	751	3.53	0.006	589	797	315	163	425	38%
		3	0.74	3000	242	789	3.26	0.006	544	797	315	159	425	38%
		2	0.79	3000	259	1618	6.26	0.006	1043	1987	357	235	796	29%
		1	0.76	3485	289	1688	5.84	0.006	974	1320	356	218	662	33%

As a conclusion, considerable reductions in Maxwell stiffness are to be expected when the influence of the damper stiffness and auxiliary elements is taken into account. The reduction is on the order of magnitude of 25%-50% of the stiffness calculated on the basis of the brace extender cross-sectional properties and

centerline length. This conclusion is supported on the reduced amount of experimental data available, and should be taken as preliminary.

3. Sensitivity of response to Maxwell stiffness

3.1 Numerical study

A numerical study is performed in order to assess the influence of the Maxwell stiffness reduction in the seismic response of systems. In the study, Moment Resisting Frames (MRF), equipped with Added Damping Systems (ADS), are subjected to a Ground Motion Set (GMS) at different intensities. Peak values of significant variables are obtained for unreduced and reduced Maxwell stiffness, and the results are compared. The study is described hereby:

3.1.1 Moment Resisting Frames (MRFs)

Two frames 3- and 5-storey high, referred to as 03D and 05D, are studied, see Fig. 2(b)(c). The frames provide lateral strength and stiffness to a building, whose floor layout is shown in Fig. 2(a). The seismic weight for each frame is 2601kN at typical storeys and 2440kN at roof. The frames are designed for gravity and wind loads, but using capacity criteria imposed by Eurocode 8 [16], namely $\Sigma M_{c,Rd} \geq 1.3\Sigma M_{b,Rd}$, where $\Sigma M_{c,Rd}$ and $\Sigma M_{b,Rd}$ represent the addition of column and beam resisting moments, considering those elements concurrent at each joint in the frame. Column sizing was adjusted iteratively ensuring a complete global mechanism in the 1st mode pushover analysis. The fundamental periods T_1 are 1.594s (03D) and 2.010s (05D).

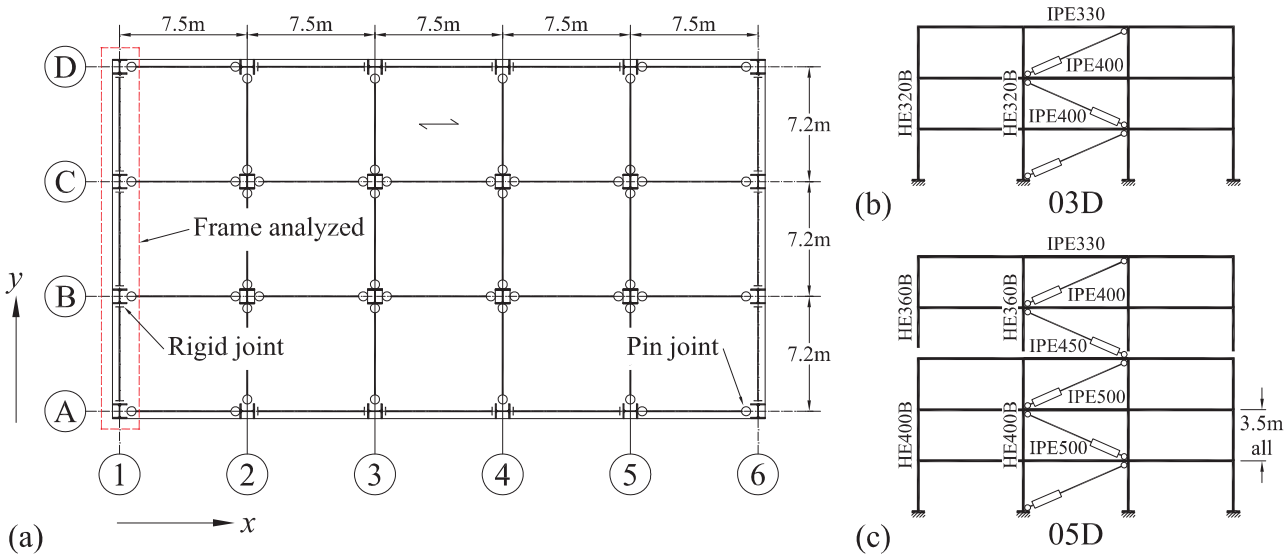

Fig. 2 – Frame definition; (a) plan layout; (b) elevation of frame 03D2; (c) elevation of frame 05D2.

3.1.2 Ground Motion Set (GMS) and seismic intensities

The frames are subjected to a set of accelerograms retrieved from the European Strong Motion Database [17] and referred to as ESB; it is formed by both horizontal components of 20 non-impulsive motions with magnitude Mw ≥ 5.5, epicentral distance between 10 km and 50 km, recorded at firm soil (ground type B as defined in Eurocode 8). The motions were individually normalized by their Peak Horizontal Acceleration (PHA) and pre-scaled so that the mean 5% elastic spectrum of the set approaches the Eurocode-defined 5% elastic response spectrum type I over a wide range of periods. Additional details can be found in [18].

Seismic intensity is measured by spectral acceleration at first mode period T_1 and 5% inherent damping $S_a(T_1,5\%)$, hereby referred to as S_{a1}. Three intensity levels, referred to as E, D, and C, are included in the study. Intensity level 'D' (from Design) is chosen to result in a maximum 2% interstorey drift on the frames, corresponding to $S_{a1,D}$ = 0.26g (frame 03D) and 0.22g (frame 05D). This condition results in a 1% interstorey drift ratio θ in damage limitation check, assuming importance class II per Eurocode 8, which is a more severe restriction than strength for these frames. $S_{a1,D}$ corresponds to Eurocode-8-defined 5% elastic spectrum anchored at PHA_D = 0.34g (03D) and 0.36g (05D), approximately. Intensity level 'C' is defined by $S_{a1,C} = 1.5S_{a1,D}$, in accordance with the relationship between design and maximum earthquakes considered in ASCE/SEI 7-16 [9]. Finally, intensity level 'E' is chosen so the frames with added damping remain elastic for all ground motions in the set. The analysis is conducted by scaling the normalized GMS to these three intensities. The median ($\hat{x}$) across ground motion responses assuming a lognormal distribution is adopted as representative.

3.1.3 Added Damping Systems (ADSs)

ADSs are included in order to obtain enhanced performance, measured as a reduction of interstorey drift ratio. ADSs are defined by a label of the type 'Q.2.1', with the following meaning:

- The first letter ('Q' in the example) indicates the height-wise distribution of damping coefficients. 'Q' corresponds to a constant distribution. 'R' and 'S' are linearly decreasing distributions with the roof coefficient taken as 2/3 or 1/3 of the first storey coefficient, respectively.
- The second digit ('2' in the example) indicates the amount of damping. Increasing values (between 1 and 3) indicate increasing amounts of damping.
- The third digit ('3' in the example) indicates the damper exponent, taken as '1' (linear) or '5' (non-linear). All dampers in an ADS are either linear or non-linear.

For frame 03D only distribution type 'Q' (constant) is used. This distribution is realistic, as actual designs tend to use a limited amount of damper types. The 'S' distribution follows loosely the vertical distribution of frame stiffness. Distributions Q.1.1, Q.2.1 and Q.3.1 present a 11%, 23% and 34% added damping ratio $\xi_{a,1}$ in the first mode for both frames, respectively. For non-linear dampers the amount of damping is displacement-dependent, therefore varies with frame and intensity level. For intensity level 'D' ($S_{a1,D}$) and frame 03D, Q.1.5, Q.2.5, and Q.3.5 correspond roughly to 13%, 29% and 46%; for $S_{a1,D}$ and frame 05D, Q.1.5, Q.2.5, and Q.3.5 correspond to 15%, 33% and 54%. The first storey damping coefficient is adjusted, so distributions type 'R' and 'S' present the same amount of added viscous damping in the first mode that the corresponding 'Q' distribution.

3.1.4 Analysis models

Analysis is performed using openSees 3.2.1 [19]. Analysis is planar and includes material and geometrical non-linearity, using force-based beam-column elements with 5 integration points, and cross sections discretized with fibers, using 12 midpoints (4 per each flange and 4 per web). No deterioration effects are included, which is deemed acceptable for the moderate ductility levels reached as a consequence of the addition of viscous damping. The Giuffré-Menegotto-Pinto hysteretic model is used. The isotropic strain hardening ratio is defined as 3% (referred to as 'PY3'). The column panel zone is assumed to be reinforced with cover plates, remaining elastic and thus is modeled with rigid links and an elastic spring with equivalent tangent stiffness. P-Δ effects are included as usual through a flexible lean-column with high axial stiffness, linked to the main structure at each level, where seismic loads are applied, minus the contributory part of the frame which is directly entered on the frame elements. Inherent damping is modeled as 2% Rayleigh damping in the 1st and 3rd mode. Time stepping was controlled by a convergence check based on a maximum 5% value of Energy Balance Error (EBE) as defined in [20].

3.1.5 Maxwell stiffness

Viscous dampers have been modeled using the openSees viscous damper material [21], defined at every storey n by damper exponent a_n, damping coefficient $c_{b,n}$, and Maxwell stiffness $k_{b,n}$. Subscript 'b' is used to indicate properties measured parallel to brace axis. The brace extenders are designed by the following process: first, an initial calculation with a very high value of stiffness ($k_{b,n}$ = 1000 kN/mm) is performed; damper forces are obtained; the brace element is designed for these forces with a 1.5 additional safety factor; in this process, only hot-finished square hollow sections (SHSH) in steel grade S355 are adopted, with a minimum wall thickness of 8mm, compact cross-sections and a reduced slenderness below 2.0 as per Eurocode 3, part 1-1 [22]. The reference values of k_b are based on the cross-sections of the designed elements and the total diagonal centerline length, and fall on the range 167 kN/mm to 367 kN/mm. Three different analysis models are generated:

- HB, with Maxwell stiffness equal to k_b.
- MB, with Maxwell stiffness equal to $0.50 \cdot k_b$, based on the upper bound of stiffness reduction.
- LB, with Maxwell stiffness equal to $0.25 \cdot k_b$, based on the lower bound of stiffness reduction.

3.2 Results

Results are obtained for the following variables: drift ratio θ; residual drift ratio θ_r; total acceleration a_t; relative input energy E_I; energy dissipated by dampers W_d; plastic strain energy dissipated by frame W_f, beams W_b and columns W_c. For space limitations, plots and tables are included hereby only for four variables closely related to damage: θ_r, W_f, θ and a_t. Each plot shows the median results of the variable of interest, obtained for analysis with the three types of Maxwell stiffness reduction considered (HB, MB, and LB). Values on Table 3 to Table 6 are averaged ratios between the median result for each variable obtained for models MB and LB (reduced stiffness) to the median result obtained for model HB (reference stiffness). Each row presents results binned according to different features of the damping system (damper exponent; amount of damping; vertical distribution of damping coefficients) or location within frames (first storey, roof). The bottom row includes all cases. The results are binned by seismic intensity (E, D, C, ALL); for variables Δ_r and W_f, intensity level E is dismissed because the frame remains essentially elastic. In these tables, each storey is considered as an independent datum.

The results are discussed for the four variables selected:

<u>Residual drift ratio</u> θ_r (see Fig. 3 and Table 3) is barely affected by the reduction in Maxwell stiffness in the 3-storey frame. In the 5-storey frame, however, this variable is largely dependent on the reduction in Maxwell stiffness. This dependency is mildly influenced by the damper type, increases with increasing damping, decreases with increasing intensity, is slightly larger for distribution type 'S', and is larger at the top half of the frame.

<u>Plastic strain energy dissipated by frame elements</u> W_f (Fig. 4 and Table 4) is strongly dependent on the reduction in Maxwell stiffness. Both frames show dependency, but it is much larger for the 5-storey frame. This dependency is stronger for non-linear dampers, increases with increasing damping, is larger for distribution type 'S', increases with increasing intensity, and is much larger at the top half of the frame.

<u>Drift ratio</u> θ (Fig. 5 and Table 5) is moderately influenced by the reduction in Maxwell stiffness. The dependency is larger for the 5-storey frame, stronger for non-linear dampers, increases with increasing damping, is not influenced by the damping coefficient distribution, decreases with increasing intensity and is much larger at the top half of the building.

<u>Total acceleration</u> a_t (Fig. 6 and Table 6) is largely affected by the reduction in Maxwell stiffness. This dependency is larger for the 5-storey frame, only mildly influenced by damper type, uninfluenced by damping coefficient distribution, decreases with increasing intensity and is much larger for the top half of the building.

Table 3 – Summary of median results: residual drift ratio.

Median $\hat{\theta}_r$				Frame 03D						Frame 05D					
ADS				MB / HB			LB / HB			MB / HB			LB / HB		
Type	Amount	*a*	Storey	D	C	ALL	D	C	ALL	D	C	ALL	D	C	ALL
ALL	ALL	1	ALL	0.98	1.01	0.99	1.00	1.00	1.00	1.30	1.19	1.25	2.53	1.79	2.16
ALL	ALL	0.5	ALL	0.98	0.98	0.98	1.19	0.98	1.08	1.13	1.08	1.11	2.23	1.52	1.87
ALL	1	ALL	ALL	0.96	1.02	0.99	1.12	1.04	1.08	1.02	0.99	1.01	1.47	1.12	1.29
ALL	2	ALL	ALL	0.98	0.98	0.98	1.01	0.91	0.96	1.14	1.13	1.13	2.29	1.61	1.95
ALL	3	ALL	ALL	1.00	0.98	0.99	1.15	1.02	1.08	1.36	1.19	1.27	3.15	2.08	2.61
Q	ALL	ALL	ALL	0.98	0.99	0.98	1.09	0.99	1.04	1.17	1.11	1.14	2.08	1.52	1.80
R	ALL	ALL	ALL	-	-	-	-	-	-	1.13	1.10	1.12	2.14	1.62	1.88
S	ALL	ALL	ALL	-	-	-	-	-	-	1.34	1.20	1.27	2.92	1.82	2.37
ALL	ALL	ALL	1	0.95	0.92	0.94	1.04	0.83	0.93	1.16	1.04	1.10	1.77	1.22	1.49
ALL	ALL	ALL	roof	1.03	1.07	1.05	1.19	1.16	1.17	1.30	1.27	1.28	3.41	2.51	2.96
ALL	ALL	ALL	ALL	0.98	0.99	0.98	1.09	0.99	1.04	1.21	1.14	1.18	2.38	1.66	2.02

Table 4 – Summary of median results: plastic strain energy dissipated by frame.

Median $\hat{W}_f$				Frame 03D						Frame 05D					
ADS				MB / HB			LB / HB			MB / HB			LB / HB		
Type	Amount	*a*	Storey	D	C	ALL	D	C	ALL	D	C	ALL	D	C	ALL
ALL	ALL	1	ALL	1.14	1.19	1.17	2.19	2.79	2.49	1.49	1.67	1.58	7.5	13.7	10.6
ALL	ALL	0.5	ALL	1.27	1.33	1.30	3.67	3.77	3.72	1.91	2.05	1.98	17.3	21.0	19.1
ALL	1	ALL	ALL	1.09	1.07	1.08	1.53	1.30	1.42	1.31	1.20	1.25	3.2	2.3	2.7
ALL	2	ALL	ALL	1.24	1.34	1.29	3.30	3.49	3.39	1.69	1.77	1.73	9.7	10.9	10.3
ALL	3	ALL	ALL	1.29	1.38	1.33	3.96	5.04	4.50	1.93	2.44	2.18	23.2	37.1	30.2
Q	ALL	ALL	ALL	1.21	1.26	1.23	2.93	3.28	3.10	1.43	1.58	1.51	6.9	12.7	9.8
R	ALL	ALL	ALL	-	-	-	-	-	-	1.60	1.70	1.65	9.5	15.0	12.3
S	ALL	ALL	ALL	-	-	-	-	-	-	2.06	2.30	2.18	20.8	24.3	22.6
ALL	ALL	ALL	1	1.02	1.03	1.03	1.38	1.18	1.28	1.18	1.08	1.13	1.9	1.4	1.7
ALL	ALL	ALL	roof	1.29	1.39	1.34	3.55	5.68	4.61	1.67	2.23	1.95	21.0	46.7	33.9
ALL	ALL	ALL	ALL	1.21	1.26	1.23	2.93	3.28	3.10	1.70	1.86	1.78	12.4	17.3	14.9

Table 5 – Summary of median results: drift ratio.

Median $\hat{\theta}$				Frame 03D								Frame 05D							
ADS				MB / HB				LB / HB				MB / HB				LB / HB			
Type	Amount	*a*	Storey	E	D	C	ALL	E	D	C	ALL	E	D	C	ALL	E	D	C	ALL
ALL	ALL	1	ALL	1.02	1.02	1.02	1.02	1.07	1.06	1.06	1.07	1.05	1.05	1.05	1.05	1.18	1.16	1.16	1.17
ALL	ALL	0.5	ALL	1.10	1.05	1.04	1.06	1.29	1.14	1.10	1.18	1.18	1.10	1.07	1.12	1.52	1.28	1.22	1.34
ALL	1	ALL	ALL	1.02	1.01	1.01	1.01	1.07	1.03	1.02	1.04	1.03	0.99	0.99	1.03	1.15	1.05	1.03	1.10
ALL	2	ALL	ALL	1.06	1.03	1.03	1.04	1.18	1.10	1.08	1.12	1.08	1.04	1.03	1.07	1.31	1.18	1.15	1.24
ALL	3	ALL	ALL	1.09	1.06	1.05	1.07	1.29	1.17	1.14	1.20	1.13	1.09	1.07	1.12	1.45	1.32	1.27	1.38
Q	ALL	ALL	ALL	1.06	1.03	1.03	1.04	1.18	1.10	1.08	1.12	1.13	1.08	1.06	1.09	1.39	1.23	1.20	1.27
R	ALL	ALL	ALL	-	-	-	-	-	-	-	-	1.11	1.07	1.06	1.08	1.33	1.22	1.18	1.25
S	ALL	ALL	ALL	-	-	-	-	-	-	-	-	1.11	1.08	1.06	1.08	1.32	1.22	1.18	1.24
ALL	ALL	ALL	1	1.02	1.01	1.01	1.01	1.09	1.05	1.04	1.06	1.05	1.03	1.02	1.04	1.21	1.14	1.10	1.15
ALL	ALL	ALL	roof	1.11	1.06	1.05	1.07	1.31	1.17	1.14	1.21	1.26	1.17	1.14	1.19	1.72	1.47	1.41	1.53
ALL	ALL	ALL	ALL	1.06	1.03	1.03	1.04	1.18	1.10	1.08	1.12	1.12	1.07	1.06	1.09	1.35	1.22	1.19	1.25

Table 6 – Summary of median results: total acceleration.

Median $\hat{a}_t$				Frame 03D								Frame 05D							
ADS				MB / HB				LB / HB				MB / HB				LB / HB			
Type	Amount	*a*	Storey	E	D	C	ALL	E	D	C	ALL	E	D	C	ALL	E	D	C	ALL
ALL	ALL	1	ALL	1.11	1.10	1.10	1.10	1.29	1.28	1.28	1.29	1.19	1.19	1.19	1.19	1.47	1.47	1.47	1.47
ALL	ALL	0.5	ALL	1.17	1.11	1.09	1.12	1.41	1.30	1.28	1.33	1.21	1.18	1.19	1.19	1.49	1.45	1.47	1.47
ALL	1	ALL	ALL	1.08	1.05	1.04	1.06	1.24	1.16	1.15	1.18	1.13	1.09	1.09	1.13	1.37	1.31	1.30	1.35
ALL	2	ALL	ALL	1.16	1.12	1.11	1.13	1.39	1.34	1.33	1.35	1.18	1.17	1.18	1.20	1.47	1.47	1.49	1.51
ALL	3	ALL	ALL	1.17	1.15	1.14	1.16	1.43	1.38	1.38	1.40	1.18	1.18	1.19	1.21	1.46	1.46	1.48	1.50
Q	ALL	ALL	ALL	1.14	1.11	1.10	1.11	1.35	1.29	1.28	1.31	1.21	1.19	1.20	1.20	1.49	1.48	1.50	1.49
R	ALL	ALL	ALL	-	-	-	-	-	-	-	-	1.20	1.19	1.19	1.19	1.48	1.47	1.48	1.48
S	ALL	ALL	ALL	-	-	-	-	-	-	-	-	1.20	1.18	1.18	1.19	1.46	1.43	1.43	1.44
ALL	ALL	ALL	1	1.07	1.06	1.06	1.06	1.21	1.18	1.16	1.18	1.05	1.05	1.05	1.05	1.15	1.13	1.11	1.13
ALL	ALL	ALL	roof	1.17	1.13	1.11	1.14	1.42	1.32	1.31	1.35	1.28	1.25	1.24	1.26	1.70	1.63	1.63	1.65
ALL	ALL	ALL	ALL	1.14	1.11	1.10	1.11	1.35	1.29	1.28	1.31	1.20	1.19	1.19	1.19	1.48	1.46	1.47	1.47

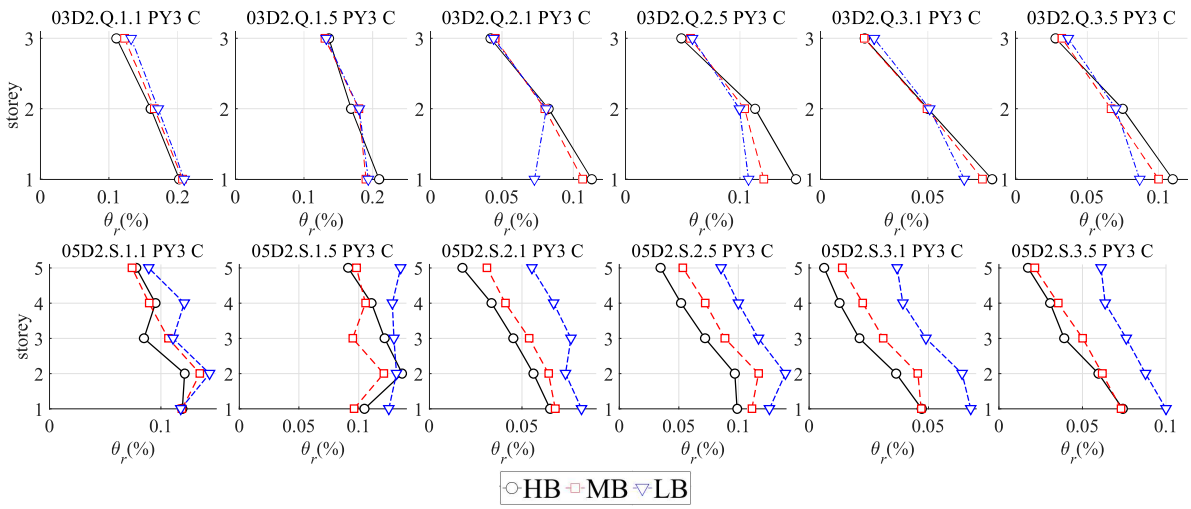

Fig. 3 – Median results for θ_r at intensity level C ($S_{a1,C}$). Frames 03D ADS Q (above), 05D ADS S (below).

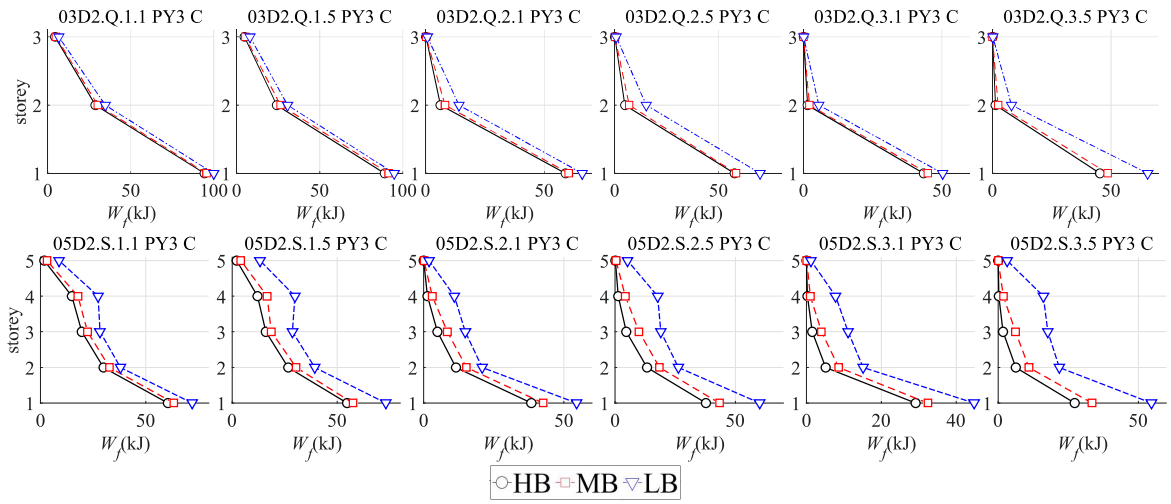

Fig. 4 – Median results for W_f at intensity level C ($S_{a1,C}$). Frames 03D ADS Q (above). 05D ADS S (below).

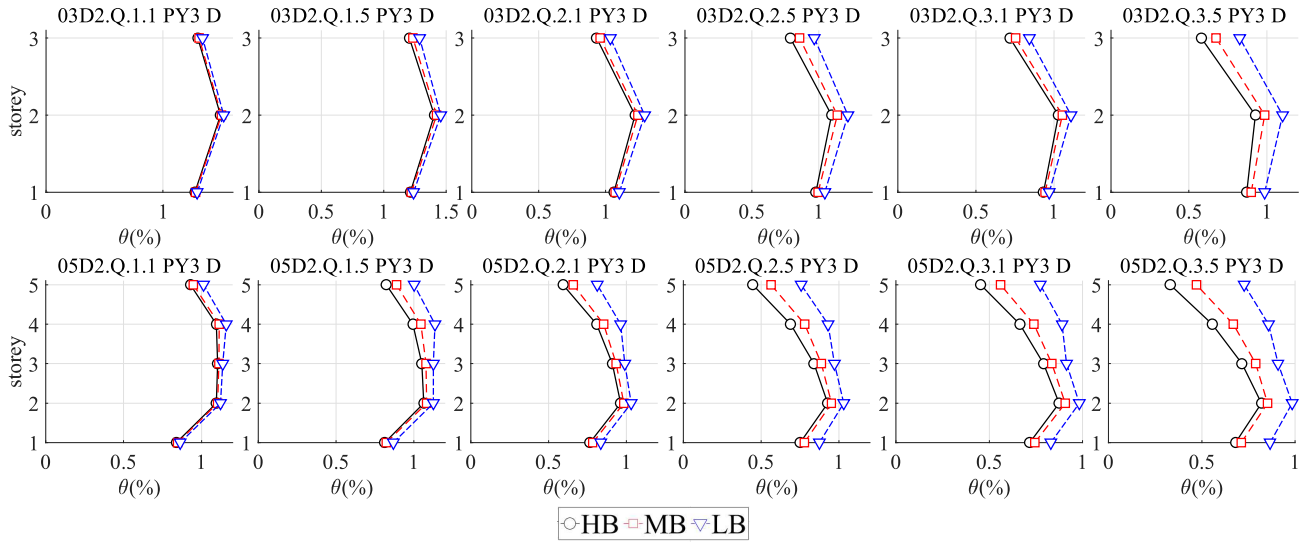

Fig. 5 – Frames 03D and 05D with ADS type Q at intensity level D ($S_{a1,D}$). Median results for θ.

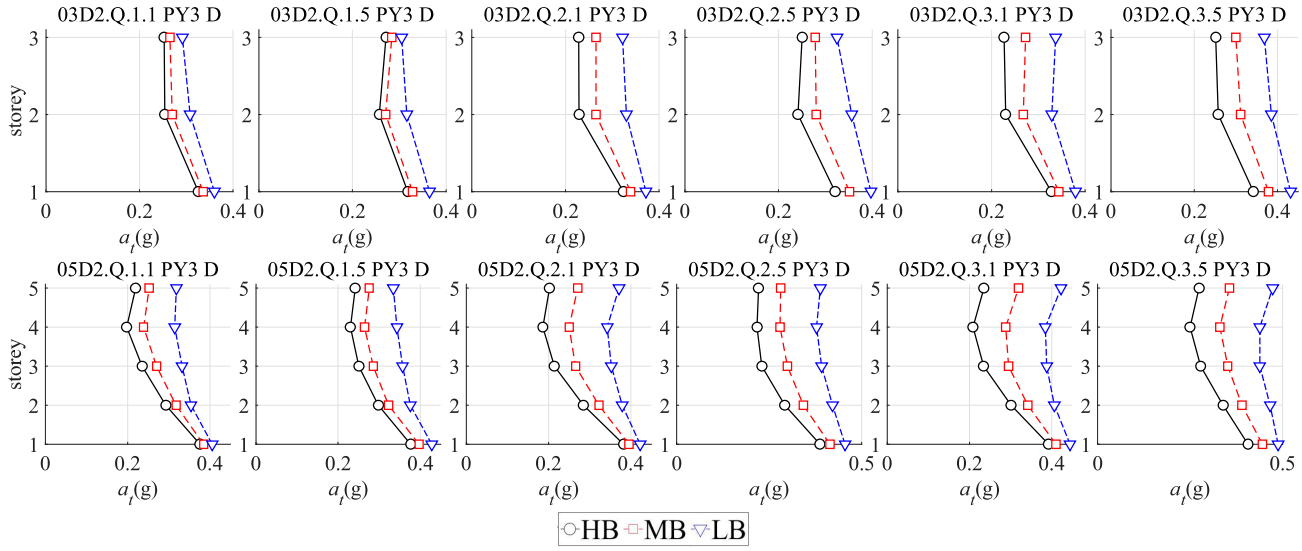

Fig. 6 – Frame 03D with Added Damping System type Q. Median results for total acceleration a_t.

A summary of results for all variables analyzed is shown in Table 7. The table includes the relative input energy E_I and energy dissipated by dampers E_d; the plastic strain energy dissipated by frame is split in its column component W_c and beam component W_b. Values on this table have been obtained as the average of MB/HB and LB/HB; for instance, the value for θ and frame 05D is obtained as the average of the values at Table 5, heading 'Frame 05D', columns 'MB/HB - ALL' and 'LB/HB – ALL'. These values (binned according to ADS properties and storey) indicate the sensitivity of each variable to the reduction in Maxwell stiffness. This sensitivity is classified as negligible (< 1.1, marked with plain text), large (≤ 1.30, highlighted in **bold red font**) and moderate (in between 1.1 and 1.30, marked with *blue italics font*).

For the 3-storey frame, W_f, W_c and W_b display a large sensitivity to the Maxwell stiffness adopted in the analysis; a_t presents a moderate sensitivity; and all other variables present a reduced or negligible sensitivity. For the 5-storey frame, W_f, W_c and W_b, θ_r and a_t display a large sensitivity; θ displays a moderate sensitivity. All variables are more affected at the top half of the building. Energy input E_I is almost unaffected by the

Maxwell stiffness. The energy dissipated by the damping system is unaffected on the average, but its vertical distribution is affected, with a reduction in dissipation at the bottom half and an increase in dissipation at the top half.

Table 7 – Summary of results.

ADS			storey	*Frame 03D*								*Frame 05D*							
Type	**Amount**	a		θ	θ_r	a_t	E_I	W_d	W_f	W_c	W_b	θ	θ_r	a_t	E_I	W_d	W_f	W_c	W_b
ALL	ALL	1	ALL	1.04	1.00	*1.20*	0.94	0.99	**1.83**	**1.47**	**1.87**	1.11	**1.70**	**1.33**	1.02	1.01	**6.1**	**3.6**	**6.2**
ALL	ALL	0.5	ALL	1.12	1.03	*1.23*	0.95	0.99	**2.51**	**1.73**	**2.57**	*1.23*	**1.49**	**1.33**	1.03	0.99	**10.5**	**3.5**	**12.0**
ALL	1	ALL	ALL	1.03	1.03	1.12	0.98	0.99	*1.25*	*1.25*	*1.19*	1.06	1.15	1.24	1.02	0.97	**2.0**	**2.0**	**2.0**
ALL	2	ALL	ALL	1.08	0.97	*1.24*	0.94	0.99	**2.34**	**1.66**	**2.32**	*1.16*	**1.54**	**1.35**	1.02	1.00	**6.0**	**2.9**	**6.3**
ALL	3	ALL	ALL	1.13	1.04	*1.28*	0.92	1.00	**2.92**	**1.90**	**3.14**	*1.25*	**1.94**	**1.35**	1.01	1.00	**16.2**	**5.4**	**18.2**
Q	ALL	ALL	ALL	1.08	1.01	*1.21*	0.95	0.99	**2.17**	**1.60**	**2.22**	*1.18*	**1.47**	**1.34**	1.02	1.00	**5.7**	**2.7**	**6.6**
R	ALL	ALL	ALL	-	-	-	-	-	-	-	-	*1.16*	**1.50**	**1.34**	1.02	1.00	**7.0**	**3.1**	**7.5**
S	ALL	ALL	ALL	-	-	-	-	-	-	-	-	*1.16*	**1.82**	**1.31**	1.03	0.99	**12.4**	**4.9**	**13.3**
ALL	ALL	ALL	1	1.04	0.93	1.12	1.04	0.88	*1.15*	*1.14*	*1.19*	1.09	**1.30**	1.09	1.10	0.74	**1.4**	**1.4**	**2.4**
ALL	ALL	ALL	roof	1.14	1.11	*1.24*	0.86	1.13	**2.98**	**1.65**	**3.23**	**1.36**	**2.12**	**1.46**	1.05	**1.40**	**17.9**	**3.0**	**19.6**
ALL	ALL	ALL	ALL	1.08	1.01	*1.21*	0.95	0.99	**2.17**	**1.60**	**2.22**	*1.17*	**1.60**	**1.33**	1.03	1.00	**8.3**	**3.6**	**9.1**

4. Conclusions

Added damping systems are formed by a damper unit and several auxiliary mounting elements, including the brace extender and other hardware. Available experimental data are used to show that the actual stiffness of the Maxwell model representing the added damping system is a reduced fraction (between 50% and 25%, approximately) of the stiffness calculated from brace extender properties and centerline length, a value commonly adopted in design. A numerical study on 3- and 5- storey frames shows that this reduction in Maxwell stiffness has a remarkable influence on several variables related to structural and non-structural damage, particularly plastic strain energy dissipated in both frames. In the 5-storey frame, residual drift ratio and total acceleration are also highly dependent on the reduction of Maxwell stiffness, and drift ratio is moderately dependent. This dependency increases with increasing damping and is larger at the top half of the building. For all variables except total acceleration this dependency is larger for non-linear dampers. For all variables except plastic strain energy the dependency decreases when the seismic intensity increases. These results suggest that, on the absence of accurate experimental information, the Maxwell stiffness used for analysis and damage estimates should be taken conservatively as a fraction (between 0.25 and 0.50, approximately) of the stiffness based on brace extender properties and centerline length. Due to the scarcity of experimental data these results should be considered as preliminary. The study considered only firm soils, and a limited number of complete vertical distributions of dampers, with emphasis on the constant vertical distribution and two exponents (linear, a = 1 and non-linear, a = 0.5). Other types of soil, taller frames, different damper distributions (including incomplete distributions) or exponents need to be investigated.

5. References

[1] Almufti, I., & REDi, W. M. (2013). Rating System: Resilience-based Earthquake Design Initiative for the Next Generation of Buildings, Version 1.0. *October, ARUP, San Francisco, CA*.

[2] Pavlou, E., & Constantinou, M. C. (2006). Response of nonstructural components in structures with damping systems. *Journal of Structural Engineering*, *132*(7), 1108-1117.

[3] Uang, C. M., & Bertero, V. V. (1988). *Use of energy as a design criterion in earthquake-resistant design* (Vol. 88). Berkeley, California: Earthquake Engineering Research Center, University of California.

[4] Gunturi, S. K. V. (1992). Building specific damage estimation. *Proc. 10WCEE*, *10*, 6001-6006.

[5] Ramirez, C. M., & Miranda, E. (2012). Significance of residual drifts in building earthquake loss estimation. *Earthquake Engineering & Structural Dynamics*, *41*(11), 1477-1493.

[6] Makris, N., Constantinou, M. C., & Reinhorn, A. M. (1990). *Viscous dampers: testing, modeling and application in vibration and seismic isolation* (pp. 1-107). Buffalo, NY: National Center for Earthquake Engineering Research.

[7] Berquist, M., De Pasquale, R., Frye, S., Gilani, A., Klembczyk, A., Lee, D., ... & Winters, C. (2019). Fluid Viscous Dampers-General Guidelines for Engineers Including a Brief History. *Taylor Devices Inc*.

[8] FEMA (2016). FEMA P-1051: 2015 NEHRP Recommended Seismic Provisions: Design Examples. *National Institute of Building Sciences, Building Seismic Safety Council, Washington, DC*, *20005*.

[9] ASCE (2017). *ASCE/SEI 7-16: Minimum design loads and associated criteria for buildings and other structures*. American Society of Civil Engineers.

[10] Kasai, K., Ito, H., Ooki, Y., Hikino, T., Kajiwara, K., Motoyui, S., ... & Ishii, M. (2010, March). Full scale shake table tests of 5-story steel building with various dampers. In *7th International Conference on Urban Earthquake Engineering (7CUEE) & 5th International Conference on Earthquake Engineering (5ICEE)* (pp. 11-22).

[11] Dong, B., Sause, R., & Ricles, J. M. (2016). Seismic response and performance of a steel MRF building with nonlinear viscous dampers under DBE and MCE. *Journal of Structural Engineering*, *142*(6), 04016023.

[12] Akcelyan, S., Lignos, D. G., Hikino, T., & Nakashima, M. (2016). Evaluation of simplified and state-of-the-art analysis procedures for steel frame buildings equipped with supplemental damping devices based on E-Defense full-scale shake table tests. *Journal of Structural Engineering*, **142** (6), 04016024.

[13] Constantinou, M. C., & Symans, M. D. (1992). *Experimental and analytical investigation of seismic response of structures with supplemental fluid viscous dampers*. Buffalo, NY: National Center for earthquake engineering research.

[14] Reinhorn, A. M., Li, C., & Constantinou, M. C. (1995). Experimental and analytical investigation of seismic retrofit of structures with supplemental damping: Part. 1-fluid viscous damping devices. In *Experimental and analytical investigation of seismic retrofit of structures with supplemental damping: Part. 1-Fluid viscous damping devices* (pp. 120-120).

[15] Seleemah, A. A., & Constantinou, M. C. (1997). *Investigation of seismic response of buildings with linear and nonlinear fluid viscous dampers*. Buffalo: National Center for Earthquake Engineering Research.

[16] CEN, (2005). Eurocode 8: Design of structures for earthquake resistance-part 1: general rules, seismic actions and rules for buildings. *Brussels: European Committee for Standardization*.

[17] Ambraseys, N., Smit, P., Douglas, J., Margaris, B., Sigbjörnsson, R., Olafsson, S., ... & Costa, G. (2004). Internet site for European strong-motion data. *Bollettino di geofisica teorica ed applicata*, *45*(3), 113-129.

[18] Conde, J. (2020). *Seismic response of structures equipped with passive energy dissipation systems using simplified methods based on equivalent effective properties*. Ph. D. dissertation, Universidad Politécnica de Madrid (UPM), Spain. DOI: 10.20868/UPM.thesis.66114.

[19] McKenna, F. (2011). OpenSees: a framework for earthquake engineering simulation. *Computing in Science & Engineering*, *13*(4), 58-66.

[20] Christopoulos, C., Filiatrault, A. (2006). *Principles of passive supplemental damping and seismic isolation*. Pavia, Italy: Iuss press.

[21] Akcelyan, S., Lignos, D. G., & Hikino, T. (2018). Adaptive numerical method algorithms for nonlinear viscous and bilinear oil damper models subjected to dynamic loading. *Soil Dynamics and Earthquake Engineering*, **113**, 488-502.

[22] CEN (2005). EN-1993-1-1:2005. Eurocode 3: Design of steel structures. Part 1-1: General rules and rules for buildings. *Brussels: European Committee for Standardization*.

